Differential cross sections for elastic electron scattering in argon over the angular range 130°–180°

Brygida Mielewska,[1] Ireneusz Linert,[1] George C. King,[2] and Mariusz Zubek[1]
[1]*Department of Physics of Electronic Phenomena, Gdansk University of Technology, 80-952 Gdansk, Poland*
[2]*Department of Physics and Astronomy, Schuster Laboratory, Manchester University, Manchester M13 9PL, United Kingdom*
(Received 25 February 2004; published 21 June 2004)

Differential cross sections for elastic electron scattering in argon have been measured in the angular range of backward scattering from 130° to 180° at incident electron energies of 5, 7.5, and 10 eV. In these measurements the magnetic angle-changing technique with a newly developed conical solenoid system has been employed. The differential cross sections measured in the above scattering angle range together with the cross sections of Gibson *et al.* [J. Phys. B **29**, 3177 (1996)] have been integrated to obtain integral elastic and momentum transfer cross sections. Detailed comparison is presented of the differential and integral cross sections obtained with the results of various theoretical calculations. The results indicate that, in general, the theoretical cross sections at the above electron energies are overestimated at the larger scattering angles.

DOI: 10.1103/PhysRevA.69.062716 PACS number(s): 34.80.Bm

I. INTRODUCTION

An exact knowledge of the differential cross section for electron scattering over the complete scattering angle range from 0° to 180° is crucial in studies of the dynamics of electron scattering from atoms and molecules. Measurements of differential cross sections for electron scattering have been most commonly performed in the angular range of forward scattering, up to typically 130°. The full angular range of backward scattering has become accessible only recently with the development of the magnetic angle-changing technique [1–3]. Differential cross sections for elastic and inelastic scattering into the backward hemisphere are provided by theoretical calculations. These theoretical data have been extensively used in extrapolation procedures to estimate integral and momentum transfer cross sections. However, as can be seen from a comparison of the calculated differential cross sections in the range of high scattering angles up to 180°, different theoretical approaches predict results that may differ by a factor of up to two. It is also interesting to note that various theoretical approaches consistently predict integral cross sections for elastic scattering that lie at or above the upper limit of the range of values obtained in the measurements of total cross sections.

The differential cross sections for elastic electron scattering in argon in the low-energy range ($\leqslant$10 eV) have been measured since the pioneering work of Ramsauer and Kollath [4] in the 1930s. The scattering angle range in their measurements was exceptionally wide and extended up to 167.5°; however, the accuracy of the measurements has not been stated and is difficult to estimate. More recent measurements of absolute differential cross sections have been carried out by Williams [5], Srivastava *et al.* [6], Weyhreter *et al.* [7], Furst *et al.* [8], and Gibson *et al.* [9] but none of these works gave the cross sections in the scattering angle range above 130°.

There has been a considerable amount of theoretical work on elastic electron scattering in argon. These works differ most significantly in their various approaches to account for long-range polarization and short-range correlation interactions in the electron scattering process, in the low energy range; they did use similar and commonly accepted ways to describe static and exchange interactions. The polarized-orbital method has been used by Thompson [10] and Garbaty and LaBahn [11] and recently by Dasgupta and Bhatia [12] to calculate elastic differential and total cross sections. McEachran and Stauffer [13] presented differential and integral cross sections calculated within their polarized-orbital method in an adiabatic exchange approximation that included a dipole polarization potential and treated exchange exactly. Very recently these authors performed relativistic calculations [14] within the general framework of their method that included multipole polarization and dynamical distortion potentials. *R*-matrix calculations for elastic scattering in argon have been carried out by Fon *et al.* [15] and Bell *et al.* [16]. In these calculations the atomic ground state was coupled with a ^1P pseudostate to include static dipole polarizability of the argon atom. The two calculations differ in the choice of the ^1P pseudostate orbital used. Saha [17] has used the multiconfigurational self-consistent-field method which was extended to include dynamical effects in the dipole polarization and electron correlation. In several theoretical investigations, advantage has been taken of the use of model potentials. Nahar and Wadehra [18] performed calculations of elastic differential cross sections using a model polarization potential with an energy-dependent adjustable parameter that was determined from a fit to the experimental cross sections. Reid and Wadehra [19] presented calculations of differential cross sections in the energy range below the lowest excitation threshold using a parameter-free model for the correlation-polarization potential. In their relativistic calculations Sienkiewicz and Baylis [20] used a model potential with two parameters to account for the dipole and quadrupole correlation polarization. Nakanishi and Schrader [21] accounted for the effects of polarization through a local adiabatic model potential that was modified by introducing a cutoff parameter. A more elaborate account of the polarization-correlation forces has been given by Gianturco and Rodriguez-Ruiz [22]. These authors used a representation of the short-range correlation forces derived from density-functional theory while preserving the polarization adiabatic approach for the long-range polarization forces. They compared their results with the calculations of O'Connell and Lane [23] who accounted for short-range correlation interaction by employing an energy-independent model potential obtained from free-electron gas theory. The compared cross sections showed significant differences in their values at high scattering angles. Haberland *et al.* [24] applied Kohn-Sham density functional theory and used an exchange-correlation potential derived from the defined correlation factors. Plenkiewicz *et al.* [25] carried out calculations using a pseudo-potential approach in which a correlation-polarization model potential was constructed by hybridization of short-range free electron gas and long-range adiabatic polarization potentials.

In the present work we have measured the differential cross sections for electron elastic scattering in the range of scattering angle from 130° to 180° and at incident electron energies of 5, 7.5, and 10 eV. The magnetic angle-changing technique [1–3] has been applied to reach these high values of scattering angle and a newly constructed conical solenoid system has been employed to produce a localized magnetic field. Absolute values of the differential cross sections have been obtained using the relative flow technique with helium as the reference gas. The main aim of these measurements was to provide the first experimental cross sections in the above angle scattering range to help resolve the discrepancies in the theoretical calculations in this angular range. In these measurements, low values of incident electron energy, ≤10 eV, have been used, since it is at these low energies that correlation and polarization interactions between the target and incident electron are expected to play dominant roles in the scattering process. Preliminary results of the present studies have been presented previously as conference contributions [26,27].

II. EXPERIMENT

The measurements have been carried out with an electrostatic electron spectrometer and a magnetic angle-changing assembly. This assembly provides a localized, static magnetic field at the interaction region that deflects the incident and scattered electrons. This allows scattering into the backward hemisphere to be measured.

The electron spectrometer has been described in detail previously [3]. It consists of a fixed electron monochromator and an electron energy analyzer that can be rotated about the target region through the angular range, $-10°$ to $120°$ with respect to the direction of the incident electron beam. The monochromator employs a hemispherical energy selector of mean radius 50 mm. Electrons leaving the energy selector are accelerated and focused onto the target gas beam by two triple-aperture lenses. Scattered electrons from the target region are decelerated and focused onto the entrance aperture of a hemispherical energy analyzer of 20 mm mean radius by a three-element cylindrical lens. Electrons transmitted by the analyzer are detected by a channel electron multiplier (Philips, type BX919). The target gas beam is produced by a single capillary of internal diameter 0.3 mm and length 10 mm. The overall energy resolution of the present measurements is 70 meV. The incident electron energy was calibrated to within ±30 meV against the position of the ^2S negative ion resonance in helium at 19.366 eV [28].

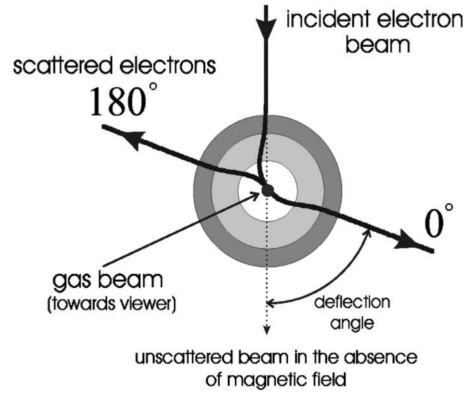

FIG. 1. Electron trajectories computed in the localized magnetic field produced by a set of inner and outer solenoids, shown in the figure by rings surrounding the scattering region. The deflection shown for the incident electron beam and scattered electrons corresponds to an electron energy of 10 eV and the inner coil's current of 0.83 A.

The magnetic angle-changing assembly has recently been described in detail by Linert *et al.* [29]. It consists of two pairs of inner and outer solenoids. The action of the solenoid assembly is illustrated in Fig. 1 which shows a cross section through the solenoids in the electron scattering plane. The magnetic field deflects the electrons that are incident on the target region and also deflects the scattered electrons by the same amount. In the present measurements the total deflection angle of the scattered electrons is 70°. Coupled with the angular range of the rotatable analyzer $(-10°$ to $120°)$ this allows the detection of scattered electrons over the full backward hemisphere, including 180°. The shape of the solenoids was chosen to be conical in the plane perpendicular to the electron scattering plane, since by suitable choice of the dimensions of this conical shape the octupole moment of the magnetic field can be cancelled. The dipole moment of the solenoid assembly was cancelled by suitable choice of the ratio of currents in the inner and outer solenoids. For the present design this ratio is equal to $1:-0.327$. (The quadrupole and 16-pole magnetic moments of the system are automatically zero in all currents systems with cylindrical symmetry.) These measures ensure a very rapid decrease of the magnetic field with radial distance. The magnetic field is uniform up to about 2 mm from the center of the target region but then decreases rapidly with radial distance, reaching 0.1% of its maximum value at a distance of 40 mm. The magnetic angle changer has the effects of slightly increasing the angular and spatial extent of the transmitted electron beam [2]. The ratio of the number of layers of turns in the inner and outer solenoids (6:4 in the present construction) was adjusted to minimize these effects. The angular scale of the present measurements was calibrated by observing the maximum in the elastic differential cross section of argon that occurs at 180°. The total uncertainty in the angular scale is estimated to be ±2° and the angular resolution is estimated to be 4°. The conical shape has the additional advantage that it provides a very open structure so that the target gas can be efficiently pumped away from the target region.

The differential cross sections for elastic scattering in argon have been measured over the angular range 130° to 180°: the magnetic angle changer produced a fixed defection angle of 70° and the electron energy analyzer was rotated about the interaction region to obtain the required 50° angular range. The yield of elastically scattered electrons in argon was measured at each scattering angle and corrected for the angular response of the electron spectrometer, simultaneously measured in helium using elastic differential cross section of Nesbet [30]. These relative elastic cross sections in argon were then made absolute by normalizing to the cross section measured at 180° using the relative flow technique [31,32] with helium as a reference gas and the calculated cross section of Nesbet [30]. The incident current was continuously measured with a Faraday cup. As a check on the procedure used, absolute values of the differential cross section were determined at additional, selected scattering angles in the region 60°–110° where comparison can be made with earlier measurements. The relative flow technique employed is similar to that used by Khakoo and Trajmar [33]. A shutoff valve was placed between the target gas capillary and the leak valve controlling the target gas flow. This provided a finite volume between these two valves and when the shutoff valve was closed the pressure in the volume rose steadily. The relative gas flows for the argon and helium gases were determined from their measured rate of pressure increases using a Baratron pressure gauge. The driving pressure of argon behind the capillary was maintained within the range 5.8–6.7 Pa. The pressure of the helium reference gas was adjusted to fulfil the requirement of equal mean free path lengths for both gases in the beam-forming capillary. This gave a ratio of driving pressures for helium and argon gases equal to 2.8.

In order to maintain high operational stability of the electron spectrometer both gases were always present simultaneously in the vacuum chamber. This was achieved by admitting one gas to the scattering region through the capillary and the other directly to the vacuum chamber through a side valve. The measured yield also contains a contribution due to background gas in the interaction region. This contribution was determined by bypassing the capillary and admitting the argon and helium gases directly into the vacuum chamber through side valves.

The quoted uncertainties in the measured values of the absolute elastic cross sections arise from the determination of the relative flow rates of argon and helium, the scattered electron yields, and the incident electron current. There is also the uncertainty in the theoretical elastic cross section for helium [30] which is quoted as 1%. From the statistical distribution of several series of measurements, the resultant uncertainty in the measured elastic differential cross sections is estimated to be 15%.

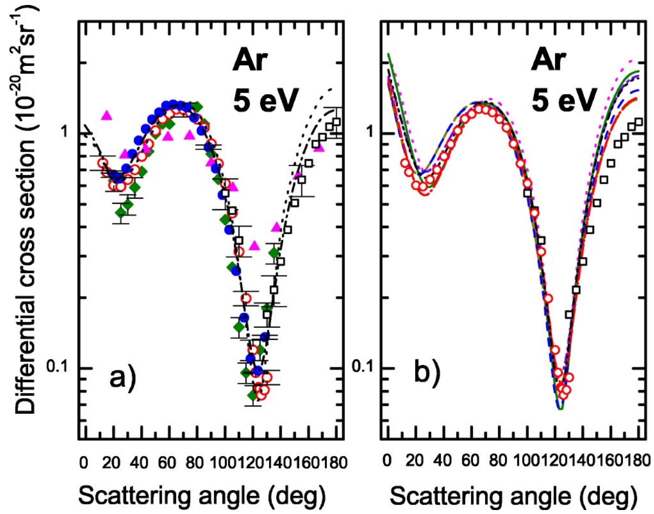

FIG. 2. (Color online) Differential cross sections for electron elastic scattering in argon at the energy of 5 eV. (a) Experimental results, □; present results, ▲; Ramsauer and Kollath [4], ○; Gibson *et al.* [9], ♦; Srivastava *et al.* [6], ●; Furst *et al.* [8]; results of phase shifts analysis, — · —, Furst *et al.* [8]; ···, Gibson *et al.* [9]; (b) experimental results, □; present results, ○; Gibson *et al.* [9]; theoretical results, ---, McEachran and Stauffer [13]; – – –, Fon *et al.* [15]; —, Saha [17]; –·–, Sienkiewicz and Baylis [20]; –··–, McEachran and Stauffer [14]; — · —, Dasgupta and Bhatia [12]; — — —, Bell *et al.* [16].

III. RESULTS AND DISCUSSION

A. Differential cross sections

The absolute differential cross sections measured in argon at electron energies of 5, 7.5, and 10 eV and over the angular range from 130° to 180° are presented in Figs. 2(a), 3(a), and 4(a), respectively. They are also listed in Table I. The additional measurements, in the range from 60° to 110°, that were undertaken to provide comparison with previous experimental data are also shown in Figs. 2(a), 3(a), and 4(a) and are included in Table I. Figures 2(b), 3(b), and 4(b) compare the results of Gibson *et al.* [9], the most recent measurements performed in the angular region 15°–130° and our results of the 130°–180° region with the results of various theoretical calculations in argon [12–17,20] which have been chosen for comparison from a number of theoretical works [10–25]. They represent various theoretical approaches used in the calculations.

The present results extend substantially the angular range of the available cross-section data in argon. They are shown together with the experimental data of Srivastava *et al.* [6], Furst *et al.* [8], and Gibson *et al.* [9], obtained for scattering angles below 130°, and with the results of Ramsauer and Kollath [4] which for 5 eV and 10 eV extend to 150° and 167.5°. These latter are the only existing data in the region of large scattering angles. For the three incident energies our differential cross sections agree favorably at 130° with the cross sections of Furst *et al.* [8] and Gibson *et al.* [9] which are consistent with each other. Our measurements at selected scattering angles below 130° also agree well with the existing differential cross sections. The cross sections of Srivas-

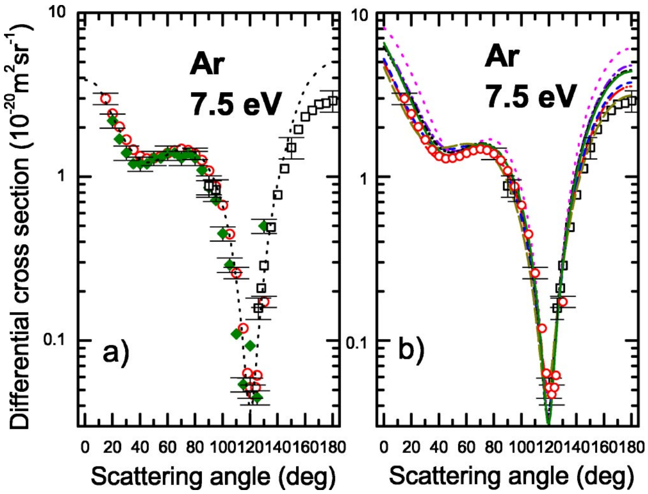

FIG. 3. (Color online) Differential cross sections for electron elastic scattering in argon at the energy of 7.5 eV. (a) Experimental results, □; present results, ○, Gibson *et al.* [9]; ♦, Srivastava *et al.* [6]; results of phase shifts analysis, ···, Gibson *et al.* [9]; (b) experimental results, □; present results, ○; Gibson *et al.* [9]; theoretical results, ---, McEachran and Stauffer [13]; – – –, Fon *et al.* [15]; —, Saha [17]; –·–, Sienkiewicz and Baylis [20]; –··–, McEachran and Stauffer [14]; — · —, Dasgupta and Bhatia [12]; — — —, Bell *et al.* [16].

tava *et al.* [6] are consistently higher in the region above the minimum which lies at about 120° and consistently lower below 120° than the results of Furst *et al.* [8] and Gibson *et al.* [9] up to about 25%. It is interesting to note that the results of Ramsauer and Kollath [4] (for 5 eV and 10 eV) are

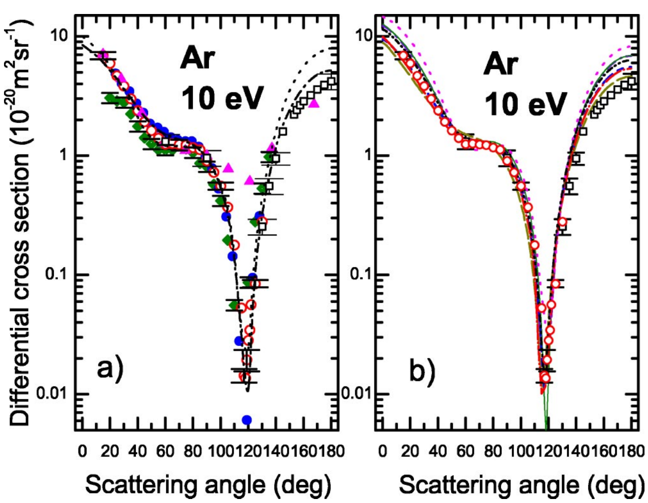

FIG. 4. (Color online) Differential cross sections for electron elastic scattering in argon at the energy of 10 eV. (a) Experimental results, □; present results, ▲; Ramsauer and Kollath [4]; ○, Gibson *et al.* [9]; ♦, Srivastava *et al.* [6]; ●, Furst *et al.* [8]; results of phase shifts analysis, –·–, Furst *et al.* [8]; ···, Gibson *et al.* [9]; (b) experimental results, □, present results; ○, Gibson *et al.* [9]; theoretical results, ---, McEachran and Stauffer [13]; – – –, Fon *et al.* [15]; —, Saha [17]; –·–, Sienkiewicz and Baylis [20]; –··–, McEachran and Stauffer [14]; — · —, Dasgupta and Bhatia [12]; — — —, Bell *et al.* [16].

TABLE I. Differential cross sections, in units of 10^{-20} m^2 sr^{-1}, for elastic electron scattering in argon at incident energies of 5, 7.5, and 10 eV.

Scattering angle (deg) \ Electron energy (eV)	5	7.5	10
60			1.32
90		0.881	0.962
95		0.832	
100	0.558		
105	0.470		
110	0.351		
126		0.158	
128		0.209	
130	0.170	0.288	0.251
135	0.225	0.493	0.558
140	0.307	0.774	0.925
145	0.390	1.12	1.60
150	0.507	1.51	
153			2.22
155	0.635	1.95	2.43
158			2.66
160	0.746	2.32	2.87
165	0.903	2.54	3.23
170	0.966	2.77	3.59
175	1.07	2.82	3.94
180	1.12	2.92	4.22

in reasonably good agreement with the present differential cross sections. In Figs. 2(a), 3(a), and 4(a) we also include, in the whole angular range 0°–180° cross sections calculated from the phase shifts determined by Furst *et al.* [8] and Gibson *et al.* [9] in the analysis of their cross sections measured in the angular range below 130°.

Comparing the experimental and theoretical cross sections it can be seen that at the energy of 5 eV, the calculated cross sections are consistently higher than the measured cross section in the angular region above 130° [Fig. 2(b)]. At 180° the calculated cross sections lie from 25% to about 90% above the experimental value. They also differ from each other by as much as a factor of 1.5. The one that differs most from our experimental result is the cross section from the early, polarized-orbital calculations of McEachran and Stauffer [13] that only included the dipole polarization interaction. Better agreement with experiment has been achieved with their very recent relativistic calculations [14] which accounts for multipole polarization and dynamical distortion. The closest to our high-angle cross sections are the results of the *R*-matrix calculations of Bell *et al.* [16] and the polarized-orbital calculations of Dasgupta and Bhatia [12]. Both include only the adiabatic dipole part of the interaction and these results almost coincide with each other. It is of note that the theoretical cross sections shown in Fig. 2(b) reproduce rather well the experimental angular dependence in the intermediate angular range 60°–130° and generally follow the experimental cross sections. However below 60° that agreement is noticeably reduced and the theoretical cross sections are more scattered with the results of Dasgupta and Bhatia [12] and Bell *et al.* [16] showing the greatest difference. It is also worth noting that in the region below 20° the theoretical cross sections display differences of the same order as that for the backward scattering near 180°. This also applies at 7.5 and 10 eV incident energy. The cross sections calculated in the region of 180° using the phase shifts of Furst *et al.* [8] and Gibson *et al.* [9] [Fig. 2(a)] also exceed our experimental values.

In Figs. 3(a) and 3(b) similar comparisons are made for the cross sections at 7.5 eV incident energy. Our differential cross section at 130° agrees with the measured value of Gibson *et al.* [9], within experimental uncertainty. The present measurement above 130° is the first result obtained in this range of scattering angle in argon. The cross section of Srivastava *et al.* [6], as at 5 eV, show differences with respect to the other measurements at scattering angles between 90° and 130° [Fig. 3(a)]. However they are in better overall accord with the results of Gibson *et al.* [9] in the region of the first minimum near 40°. Figure 3(b) indicates that for high scattering angles, as in the case of 5 eV, the theoretical calculations predict absolute differential cross sections that are higher than our experimental values by up to 100% in the case for the earlier work of McEachran and Stauffer [13]. The exception again is the *R*-matrix result of Bell *et al.* [16], whose cross section is in very good agreement with the present measurement. However, around 40°–50°, the cross section of Bell *et al.* [16] deviates from the experimental results more than the other theoretical calculations. The cross section obtained from the phase shift analysis of Gibson *et al.* [9] [Fig. 3(a)], reproduces very well the experimental results below 130°, but at 180° is 30% higher than the present measurement.

At the incident electron energy of 10 eV our cross section at 130° and our additional measurements at 60° and 90° are in good agreement with the results of Furst *et al.* [8] and Gibson *et al.* [9] which, in turn, are consistent with each other [Fig. 4(a)]. As for the cases of 5 eV and 7.5 eV incident energy, the theoretical results [Fig. 4(b)], tend to overestimate the cross sections for high scattering angles, when compared with our measurements. Again, the *R*-matrix calculations of Bell *et al.* [16] provide results which are close (within 9% at 180°) to our high-angle cross sections. At this energy they are also in good accord with the lower angle measurements of Gibson *et al.* [9]. The scatter of the theoretical cross sections at 180° is still as high as for the other two electron energies with the cross section of McEachran and Stauffer [13] giving the largest value. The cross sections obtained using the phase shift analysis of Furst *et al.* [8] and Gibson *et al.* [9] give values that at 180° are 23% and 55%, respectively, higher than our experimental result [Fig. 4(a)].

B. Integral and momentum transfer cross sections

The integral elastic cross section σ_t and the momentum transfer cross section σ_m at the three studied energies have been deduced from integration of the differential cross sections over the total angular range 0°–180°. For the angular range 15°–130°, the cross sections of Gibson *et al.* [9] were taken. For the angular range 130°–180°, the present cross sections were used. For the angular range 0°–15°, the results of Gibson *et al.* were extrapolated, using their phase shifts obtained in fitting the 15°–130° cross section.

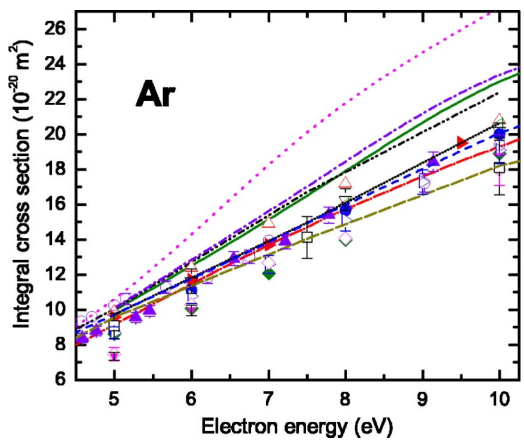

FIG. 5. (Color online) Integral cross sections for elastic electron scattering in argon, □, present results; total cross section measurements, ▼; Sinapius *et al.* [34], △, Jost *et al.* [35]; ♦, Ferch *et al.* [36]; ●, Buckman and Lohmann [37]; ▶, Kaupila *et al.* [38]; ◁, Nickel *et al.* [43]; ▷, Szmytkowski *et al.* [42]; ○, Charlton *et al.* [39]; ▲, Subramanian and Kumar [40]; ◇, Golden and Bandel [41]; ▽, Baek and Grosswendt [44]; theoretical integral cross sections, ---, McEachran and Stauffer [13]; – – –, Fon *et al.* [15]; —, Saha [17]; –·–, Sienkiewicz and Baylis [20]; –··–, McEachran and Stauffer [14]; — · —, Dasgupta and Bhatia [12]; — — —, Bell *et al.* [16]; integral cross sections from phase shift fitting, ···, Gibson *et al.* [9].

The integrated cross sections obtained at 5, 7.5, and 10 eV are compared with the results of total cross-section measurements [34–44] and calculated integral cross sections [12–17,20] in Fig. 5. The deduced momentum transfer cross sections are shown in Fig. 6 together with the calculated cross sections [12–17,20] and the cross sections obtained from swarm experiments [45–47]. The present integral and momentum transfer cross sections are also listed in Table II together with their associated uncertainties. The uncertainties in the integral and momentum transfer cross sections are less than 8.5% and 11.5%, respectively, and result from the uncertainties in the differential cross sections of Gibson *et al.* (typically around 7%) and in the present work (15%). The uncertainty arising from the extrapolated cross section (0°–15° range) contributes less than 1% to the total uncertainty.

Our integrated cross section is in very good agreement with the measurements of the total cross section, as can be seen in Fig. 5. In particular our results at 5 eV and at 7.5 eV are within 3% of the recent measurements of Buckman and Lohmann [37] and Szmytkowski *et al.* [42] that are the most accurate available. For all three energies our integrated cross-section values are also within 3% of the average of the existing experimental total cross sections. The integral cross sections obtained in the theoretical calculations [12–17,20]

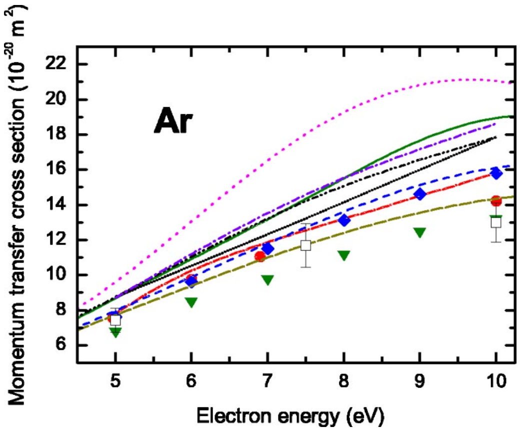

FIG. 6. (Color online) Momentum transfer cross sections in argon, □, present results; experimental cross sections, ▼ , Frost and Phelps [45]; ◆, Nakamura and Kurachi [46]; ●, Suzuki *et al.* [47]; theoretical cross sections: ---, McEachran and Stauffer [13]; – – –, Fon *et al.* [15]; —, Saha [17]; –·–, Sienkiewicz and Baylis [20]; –··–, McEachran and Stauffer [14]; — · —, Dasgupta and Bhatia [12]; — — —, Bell *et al.* [16]; cross sections from phase shift fitting, ···, Gibson *et al.* [9].

are, in general, higher than the average of the experimental ones and also higher than our deduced integral cross section. This difference increases with increasing electron energy. Of the above theoretical works, the *R*-matrix calculations of Bell *et al.* [16] and the polarized-orbital calculations Dasgupta and Bhatia [12] predict the lowest values of integral cross sections which, in fact, coincide with the present determinations. The low integral cross sections of Bell *et al.* [16] appear to arise because they overestimate the cross section over the range 30°–70°, and underestimate it over the range 70°–110°, when compared with the results of Gibson *et al.* [see Figs. 2(b)–4(b)]. The differences between the integral cross sections of Dasgupta and Bhatia [12] at 7.5 and 10 eV and our deduced cross sections is due to differences in the differential cross sections at high scattering angles. Their results below 130° are in very good agreement with the experimental cross sections. The same comment applies to the cross sections of Fon *et al.* [15] which are at the higher limit but still within the range of the total cross-section experimental values. Several of the theoretical cross sections, e.g., Refs. [13,14,17,20] lie noticeably above the range of experimental values. This is because they predict higher differential cross sections over the whole angular range. Figure 5 also presents integral cross section deduced from the phase shifts of Gibson *et al.* [9]. These two integral cross sections are

TABLE II. Integral cross section σ_t and momentum transfer cross section σ_m, in units of 10^{-20} m^2, for elastic electron scattering in argon at incident energies of 5, 7.5, and 10 eV.

Energy (eV)	σ_t	σ_m
5	9.10 ± 0.72	7.43 ± 0.68
7.5	14.1 ± 1.2	11.7 ± 1.3
10	18.4 ± 1.6	12.9 ± 1.5

above our integrated results as may be expected from the discussion of their differential cross sections [Figs. 2(a), 3(a), and 4(a)].

In Fig. 6 our deduced momentum transfer cross section is compared with that derived from swarm experiments [45–47] and that obtained from theoretical calculations [12–17,20]. The present cross sections at 5 eV and at 7.5 eV are in good agreement (to better than 10%) with the three previous experimental determinations of the momentum transfer cross section. At 10 eV our cross section is closer to the results of Frost and Phelps [45] and Suzuki *et al.* [47] (to within 2% and 8%, respectively) than to that of Nakamura and Kurachi [46] (22% difference). The momentum transfer cross sections obtained from the theoretical calculations [12–17,20] are again generally above the four experimental results, with the exception of the cross sections of Bell *et al.* [16] and Dasgupta and Bhatia [12]. These differences between the experimental and theoretical results are particularly strong in the energy region above 7 eV. The theoretical momentum transfer cross sections also show larger differences from each other than in the case of the theoretical integral cross sections. It is of note that the momentum transfer cross section of Gibson *et al.* [9] also exceed the present result.

Scattering into the backward hemisphere does, by definition introduce higher partial contribution to the momentum transfer cross section than it does to the integral cross section. For example, we find that at 7.5 and 10 eV electron energies, scattering into the region 130°–180° gives 46% and 54% contributions, respectively, into our deduced momentum transfer cross section, while these contributions to the integral cross sections are both equal to 20%. We also note that the disagreement between the calculated and experimental momentum transfer cross-sections results from overestimations of the differential cross sections for high scattering angles in the calculations. Integration of the theoretical differential cross sections over the 0°–130° range produces values that are comparable to those obtained by integrating of the experimental results of Gibson *et al.* [9], extrapolated down to 0°. At 5 eV the theoretical values are within 3.5% of the experimental value of Gibson *et al.*, and within 14.5% at 10 eV. On the other hand, similar integration of the theoretical cross sections over the 130°–180° angular range gives values that exceed the values obtained by integrating the present results over the same range. The differences are 24–50 % at 5 eV and 23–73 % at 10 eV. (This does not include the earlier results of McEachran and Stauffer [13] which show even higher differences.) Thus it is apparent that overestimation of the differential cross sections for scattering in the backward direction is the main source of the high theoretical momentum transfer cross sections. This underlines the importance of accurate determination of the differential cross section in the backward scattering direction.

IV. CONCLUSIONS

The present differential cross sections in argon, obtained at electron energy of 7.5 eV, are the first and presently the only experimentally measured cross sections in the angular range of backward scattering 130°–180°. Moreover the results obtained at energies of 5 and 10 eV are the first measured cross sections close to 180°. We have performed a comparison of the existing theoretical results with the experimental cross sections over the range, 15°–180°. In general, the theoretical results lie above the present measurements for high scattering angles. This also applies to the cross sections derived from the phase shift analysis of the cross sections measured over the low and intermediate scattering angle range (15°–130°). Further it is noticable that the theoretical differential cross sections, calculated using different theoretical approximations, are in fair agreement with each other over the range of intermediate scattering angles. However they display significant differences in the region of high scattering angles.

We have also determined the elastic integral and momentum transfer cross sections from integration of the present differential cross sections (130°–180°) and those of Gibson *et al.* [9] (15°–130° extrapolated down to 0°). The deduced cross sections show good agreement with the measured total cross sections and momentum transfer cross sections derived from electron swarm data, respectively. On the other hand, theoretical integral and momentum transfer cross sections from various theoretical approaches are higher than the average of these experimental cross sections. We suggest that the above inconsistencies between experimental and theoretical cross sections are a result of overestimation of the differential cross sections for high-angle electron scattering in the theoretical calculations. These inconsistencies are particularly evident for the case of the momentum transfer cross sections.

Similar discrepancies between theory and experiment at high scattering angles (130°–180°) have been encountered by Cho *et al.* [48] in their measurements of differential cross sections for elastic electron scattering in krypton. For example at 10 eV incident energy, the calculated 180° differential cross sections of Sienkiewicz and Baylis [49] and McEachran and Stauffer [50] are higher by 20% and 60%, respectively, than the measured value.

It is generally accepted that polarization-correlation interaction plays an important role in electron scattering in the backward direction. Gianturco *et al.* [22] have discussed various treatments of polarization-correlation interaction in the case of electron scattering by atoms of noble gases (helium to argon). They have shown that at low electron energies and high scattering angles, the cross sections may be predicted to have similar angular dependences, but their absolute values may differ significantly depending on the approximation used. The discrepancies observed in this work between the measured cross sections and the results of various theoretical approaches may be thus ascribed to difficulties in modeling the polarization-correlation interaction.

In conclusion, we hope that our work will stimulate further experimental and theoretical studies of the differential cross sections of the noble gases to resolve the existing inconsistencies and determine the relative importance of the various interaction involved in the electron scattering process.

ACKNOWLEDGMENTS

This work has been partially supported by the Polish State Committee for Scientific Research and by the Engineering and Physical Sciences Research Committee of the UK.

[1] M. Zubek, N. Gulley, G. C. King, and F. H. Read, J. Phys. B **29**, L239 (1996).
[2] F. H. Read and J. M. Channing, Rev. Sci. Instrum. **67**, 2372 (1996).
[3] M. Zubek, B. Mielewska, J. M. Channing, G. C. King, and F. H. King, J. Phys. B **32**, 1351 (1999).
[4] C. Ramsauer and R. Kollath, Ann. Phys. (Leipzig) **12**, 529 (1932).
[5] J. F. Williams, J. Phys. B **12**, 265 (1979).
[6] S. K. Srivastava, H. Tanaka, A. Chutjian, and S. Trajmar, Phys. Rev. A **23**, 2156 (1981).
[7] M. Weyhreter, B. Barzick, A. Mann, and F. Linder, Z. Phys. D: At., Mol. Clusters **7**, 333 (1988).
[8] J. E. Furst, D. E. Golden, M. Mahgerefteh, J. Zhou, and D. Mueller, Phys. Rev. A **40**, 5592 (1989).
[9] J. C. Gibson, R. J. Gulley, J. P. Sullivan, S. J. Buckman, V. Chan, and P. D. Burrow, J. Phys. B **29**, 3177 (1996).
[10] D. G. Thompson, Proc. R. Soc. London, Ser. A **294**, 160 (1966).
[11] E. A. Garbaty and R. W. LaBahn, Phys. Rev. A **4**, 1425 (1971).
[12] A. Dasgupta and A. K. Bhatia, Phys. Rev. A **32**, 3335 (1985).
[13] R. P. McEachran and A. D. Stauffer, J. Phys. B **16**, 4023 (1983).
[14] R. P. McEachran and A. D. Stauffer, Aust. J. Phys. **50**, 511 (1997).
[15] W. C. Fon, K. A. Berrington, P. G. Burke, and A. Hibbert, J. Phys. B **16**, 307 (1983).
[16] K. L. Bell, N. S. Scott, and M. A. Lennon, J. Phys. B **17**, 4757 (1984).
[17] H. P. Saha, Phys. Rev. A **43**, 4712 (1991).
[18] S. N. Nahar and J. M. Wadehra, Phys. Rev. A **35**, 2051 (1987).
[19] D. D. Reid and J. M. Wadehra, Phys. Rev. A **50**, 4859 (1994).
[20] J. E. Sienkiewicz and W. E. Baylis, J. Phys. B **20**, 5145 (1987).
[21] H. Nakanishi and D. M. Schrader, Phys. Rev. A **34**, 1823 (1986).
[22] F. A. Gianturco and J. A. Rodriguez-Ruiz, Phys. Rev. A **47**, 1075 (1993).
[23] J. K. O'Connell and N. F. Lane, Phys. Rev. A **27**, 1893 (1983).
[24] R. Haberland, L. Fritsche, and J. Noffke, Phys. Rev. A **33**, 2305 (1986).
[25] B. Plenkiewicz, P. Plenkiewicz, and J.-P. Jay-Gerin, Phys. Rev. A **38**, 4460 (1988).
[26] M. Zubek, B. Mielewska, I. Linert, and G. C. King, in Proceedings of International Symposium on Electron-Molecule Collisions and Swarms, Prague, Czech Republic, 2003, p. 1.
[27] M. Zubek, in Proceedings of SPIE—the International Society

of Optical Engineering, IV. Workshop on Atomic and Molecular Physics, Jurata, Poland 2002, Vol. 5258, 82.
[28] J. N. H. Brunt, G. C. King, and F. H. Read, J. Phys. B **10**, 1289 (1977).
[29] I. Linert, G. C. King, and M. Zubek, J. Electron Spectrosc. Relat. Phenom. **134**, 1 (2004).
[30] R. K. Nesbet, Phys. Rev. A **20**, 58 (1979).
[31] S. K. Srivastava, A. Chutjian, and S. Trajmar, J. Chem. Phys. **63**, 2659 (1975).
[32] J. C. Nickel, P. W. Zetner, G. Shen, and S. Trajmar, J. Phys. E **22**, 730 (1989).
[33] M. A. Khakoo and S. Trajmar, Phys. Rev. A **34**, 138 (1986).
[34] G. Sinapius, W. Raith, and W. G. Wilson, J. Phys. B **13**, 4079 (1980).
[35] K. Jost, P. G. F. Bisling, F. Eschen, M. Felsmann, and L. Walther, in *Proceedings of the 13th International Conference on the Physics of Electronic and Atomic Collisions*, edited by J. Eichler (North-Holland, Amsterdam, 1983), p. 91.
[36] J. Ferch, B. Granitza, C. Masche, and W. Raith, J. Phys. B **18**, 967 (1985).
[37] S. J. Buckman and B. Lohmann, J. Phys. B **19**, 2547 (1986).
[38] W. E. Kaupila, T. S. Stein, G. Jesion, and M. S. Dababneh, Rev. Sci. Instrum. **48**, 822 (1977).
[39] M. Charlton, T. C. Griffith, G. R. Heyland, and T. R. Twomey, J. Phys. B **13**, L239 (1980).
[40] K. P. Subramanian and V. Kumar, J. Phys. B **20**, 5505 (1987).
[41] D. E. Golden and H. W. Bandel, Phys. Rev. **149**, 58 (1966).
[42] C. Szmytkowski, K. Maciag, and G. Karwasz, Phys. Scr. **54**, 271 (1996).
[43] J. C. Nickel, K. Imre, D. F. Register, and S. Trajmar, J. Phys. B **18**, 125 (1985).
[44] W. Y. Baek and B. Grosswendt, J. Phys. B **36**, 731 (2003).
[45] L. S. Frost and A. V. Phelps, Phys. Rev. **136**, A1538 (1964).
[46] Y. Nakamura and M. Kurachi, J. Phys. D **21**, 718 (1988).
[47] M. Suzuki, T. Taniguchi, and H. Tagashira, J. Phys. D **23**, 842 (1990).
[48] H. Cho, R. J. Gulley, and S. J. Buckman, J. Korean Phys. Soc. **42**, 71 (2003).
[49] J. E. Sienkiewicz and W. E. Baylis, J. Phys. B **25**, 2081 (1992).
[50] R. P. McEachran and A. D. Stauffer, J. Phys. B **36**, 3977 (2003).